

Supplement of Atmos. Chem. Phys., 21, 3317–3343, 2021
<https://doi.org/10.5194/acp-21-3317-2021-supplement>
© Author(s) 2021. This work is distributed under
the Creative Commons Attribution 4.0 License.



Supplement of

**Model physics and chemistry causing intermodel
disagreement within the VolMIP-Tambora
Interactive Stratospheric Aerosol ensemble**

Margot Clyne et al.

Correspondence to: Margot Clyne (margot.clyne@colorado.edu)

The copyright of individual parts of the supplement might differ from the CC BY 4.0 License.

Supplementary Info

S1 Derivation of Eqs. (1 and 2)

1175 This section shows how we adapted equations from Seinfeld and Pandis (2016) to derive our Eqs. (1 and 2). Arising from *Beer-Lambert law*, the generic optical depth is the integral of the extinction coefficient (b_{ext}) over a path (e.g. through the atmosphere) (e.g. Seinfeld and Pandis 2016 Eq. (4.13)). Assuming a constant b_{ext} over a path of length z gives the layer optical depth (τ):

$$\tau = b_{ext} z \quad (S1)$$

The extinction coefficient for a given wavelength (λ) for particles ranging in diameter (D_p) from 0 to D_{pmax} is defined as:

$$1180 \quad b_{ext} = \int_0^{D_{pmax}} E_{ext}(D_p, \lambda, m) n_M(D_p) dD_p \quad (S2, \text{Seinfeld and Pandis 2016 Eq. (15.40)})$$

where E_{ext} is the mass extinction efficiency (with function parameters of particle size, wavelength, and complex refractive index (m)), and $n_M(D_p)$ is the mass size distribution. The total mass of particles of all sizes per volume (m_p) is:

$$m_p = \int_0^{D_{pmax}} n_M(D_p) dD_p \quad (S3)$$

So by the Mean Value Theorem for definite integrals, the mean value over the mass size distribution of the mass extinction efficiency, $\langle E_{ext} \rangle$, is:

$$\langle E_{ext} \rangle = \frac{\int_0^{D_{pmax}} E_{ext}(D_p, \lambda, m) n_M(D_p) dD_p}{\int_0^{D_{pmax}} n_M(D_p) dD_p} = \frac{1}{m_p} \int_0^{D_{pmax}} E_{ext}(D_p, \lambda, m) n_M(D_p) dD_p = \frac{1}{m_p} b_{ext} \quad (S4)$$

So,

$$b_{ext} = \langle E_{ext} \rangle m_p \quad (S5)$$

The mass extinction efficiency for spherical particles is:

$$1190 \quad E_{ext}(m, D_p, \lambda) = \frac{3}{2 \rho_p D_p} Q_{ext}(m, \alpha) \quad (S6, \text{Seinfeld and Pandis 2016 Eq. (15.41)})$$

which comes from the dimensionless extinction efficiency of a particle (Q_{ext}) as a function of complex refractive index (m) and optical size parameter ($\alpha = \frac{\pi D_p}{\lambda}$), and the ratio of cross sectional area to mass ($\frac{3}{2 \rho_p D_p}$) where ρ_p is the particle density. Maintaining the notation of “< brackets >” to denote the mean value over the mass size distribution:

$$\langle E_{ext} \rangle = \left\langle \frac{3}{2 \rho_p D_p} Q_{ext} \right\rangle \quad (S7)$$

1195 For a monodisperse population (e.g. if the aerosols were of uniform size), Eq. (S7) would simply be:

$$\langle E_{ext} \rangle = \frac{3}{4 \rho_p r_p} Q_{ext}(m, \alpha) = E_{ext} \quad (S8)$$

where r_p is the particle radius. However, since the aerosols are polydisperse, we must account for the different sizes of the aerosols in Eq. (S7). By the proof in the subsequent section (Sect. S1.1), we have:

$$\langle \rho_p r_p \rangle = \langle \rho_p \rangle r_{eff} \quad (S9)$$

1200 And if we assume:

$$\langle Q_{ext}(m, \alpha(\lambda, r_p)) \rangle \approx Q_{ext}(m, \alpha(\lambda, r_{eff})), \text{ which we denote as } Q_{ext}(r_{eff}) \quad (S10)$$

Equation (S7) becomes:

$$\langle E_{ext} \rangle = \frac{3}{4(\rho_p)r_{eff}} \langle Q_{ext}(m, \alpha) \rangle \quad (\text{by Eq. (S9)}) \quad (\text{S11a})$$

$$\simeq \frac{3}{4(\rho_p)r_{eff}} Q_{ext}(r_{eff}) \quad (\text{by Eq. (S10)}) \quad (\text{S11b})$$

1205 We note that the approximate equation for polydisperse aerosol, Eq. (S11b), becomes exact for monodisperse aerosol.

The mass extinction efficiency ($E_{ext}(m, D_p, \lambda)$) can be written in units of [$\text{m}^2 / \text{g SO}_4^{2-}$] for sulfate-containing particles by writing the particle density (ρ_p) in units of [$\text{g SO}_4^{2-} / \text{m}^3$]. The mass extinction efficiency is the same as the mass scattering efficiency for sulfate aerosols because there is no absorption. Seinfeld and Pandis (2016) write this mass extinction efficiency as $\alpha_{SO_4^{2-}}$ (not to
1210 be confused with the notation for the optical size parameter in Eqs. (S6 to S11a)) and call it the light-scattering mass efficiency of the aerosol for sulfate-containing particles. For a sulfate aerosol layer of vertical pathlength H (m), the aerosol optical depth (τ) in Seinfeld and Pandis (2016) is expressed as Eq. (S12), which comes from Eq. (S1).

$$\tau = \alpha_{SO_4^{2-}} m_{SO_4^{2-}} H \quad (\text{S12, Seinfeld and Pandis 2016 Eq. (24.24)})$$

where $m_{SO_4^{2-}}$ is the mass aerosol concentration in units of [$\text{g SO}_4^{2-} / \text{m}^3$] (not to be confused with the notation for the complex
1215 refractive index in Eqs. (S2 to S11a)). The mean column aerosol optical depth ($\bar{\tau}$) (which in our case is the stratospheric optical depth), is similarly expressed in Seinfeld and Pandis (2016) as:

$$\bar{\tau} = \alpha_{SO_4^{2-}} \overline{m_{SO_4^{2-}}} \quad (\text{S13, Seinfeld and Pandis 2016 Eq. (24.27)})$$

where $\overline{m_{SO_4^{2-}}}$ is the column burden of sulfate aerosol in units of [$\text{g SO}_4^{2-} / \text{m}^2$].

1220 The expressions pulled from Seinfeld and Pandis (2016) thus far have been describing the dehydrated sulfate aerosol. Sulfuric acid particles are always hydrated, so we need to account for the water component of the sulfate aerosol in our expression for aerosol optical depth. Seinfeld and Pandis (2016) do this by scaling $\alpha_{SO_4^{2-}}$ by a factor which is a function of relative humidity to account for the change in the scattering cross section with the presence of water (Seinfeld and Pandis, 2016 Eq. (24.25)). We use the following method instead. Equation (S6), which is Eq. (15.41) in Seinfeld and Pandis (2016), is given in terms of the particle
1225 component of the aerosol only, but we can convert to the full wet sulfate aerosol ($\text{H}_2\text{O}-\text{H}_2\text{SO}_4$) by using the mean wet particle radius (which is the effective radius, R_{eff}) instead of the dry particle diameter, D_p , and using the density, ρ , of the full wet sulfate aerosol [$\text{g H}_2\text{O}-\text{H}_2\text{SO}_4 / \text{m}^3$] instead of just the density of the sulfate particle component, ρ_p , [$\text{g SO}_4^{2-} / \text{m}^3$]. We also want our equation in terms of the column mass burden of S, because we are tracking the mass of S in the model outputs instead of tracking the mass of SO_4^{2-} . Thus, we write:

$$1230 \quad AOD = \alpha_S \frac{M}{A} \quad (\text{S14})$$

where α_S is the aerosol mass extinction coefficient in units of [$\text{m}^2 / \text{g S}$], and M and A are the stratospheric mass burden of sulfate aerosol and surface area of the Earth, giving the second term units of [$\text{g S} / \text{m}^2$]. These quantities are related to those in Eq. (S13, Seinfeld and Pandis 2016 Eq. (24.27)) by:

$$\frac{M}{A} = \overline{m_{SO_4^{2-}}} \frac{(\text{molec.weight S})}{(\text{molec.weight } SO_4^{2-})} \quad (\text{S15a})$$

$$1235 \quad \alpha_S = \frac{3 Q_{ext} (\text{molec. weight } H_2SO_4) [H_2O-H_2SO_4]}{4 \rho_{Reff} (\text{molec. weight } S) [H_2SO_4]} = \frac{3 q (\text{molec. weight } H_2SO_4)}{4 \rho_{Reff} (\text{molec. weight } S) \omega} \quad (S15b)$$

Rearranging gives our derived Eqs. (1 and 2) from the main text:

$$\psi = \frac{3q (\text{molec. weight } H_2SO_4)}{4\rho A (\text{molec. weight } S) * \omega} \quad (2)$$

and

$$AOD = \psi * \frac{M}{Reff} \quad (1)$$

1240 S1.1 Proof of Eq. (S9)

The mass size distribution (n_M) for spherical particles of diameter D_p is related to the number size distribution (n) by:

$$n_M(D_p) = \frac{\pi}{6} \rho_p D_p^3 n(D_p) \quad (S16, Seinfeld and Pandis 2016 Eq. (8.8))$$

So,

$$n(r_p) = \frac{3}{4\pi \rho_p r_p^3} n_M(r_p) \quad (S17)$$

1245 recall from Appendix A that:

$$r_{eff} = \frac{\int_{r_{min}}^{r_{max}} r \pi r^2 n(r) dr}{\int_{r_{min}}^{r_{max}} \pi r n(r) dr} \quad (A2)$$

Plugging in Eq. (S17) and assuming for now that r_p can be substituted for r yields:

$$r_{eff} = \frac{\frac{3}{4\pi} \int_{r_{min}}^{r_{max}} \frac{\pi r_p^2}{\rho_p r_p^3} n_M(r_p) dr_p}{\int_{r_{min}}^{r_{max}} \frac{\pi r_p^2}{\rho_p r_p^3} n_M(r_p) dr_p} = \frac{\int_{r_{min}}^{r_{max}} \frac{1}{\rho_p} n_M(r_p) dr_p}{\int_{r_{min}}^{r_{max}} \frac{1}{\rho_p r_p} n_M(r_p) dr_p} \quad (S18)$$

1250 All of the integrals in Eqs. (S18 and S19) are actually definite integrals (i.e. bounded by the minimum and maximum radius values defined in the model's size distribution). Applying the Mean Value Theorem for definite integrals to Eq. (S18) yields:

$$r_{eff} = \frac{\int_{r_{min}}^{r_{max}} \frac{1}{\rho_p} n_M(r_p) dr_p}{\int_{r_{min}}^{r_{max}} n_M(r_p) dr_p} * \frac{\int_{r_{min}}^{r_{max}} n_M(r_p) dr_p}{\int_{r_{min}}^{r_{max}} \frac{1}{\rho_p r_p} n_M(r_p) dr_p} = \frac{\langle \frac{1}{\rho_p} \rangle}{\langle \frac{1}{\rho_p r_p} \rangle} = \frac{\langle \rho_p r_p \rangle}{\langle \rho_p \rangle} \quad (S19)$$

therefore,

$$\langle \rho_p \rangle r_{eff} = \langle \rho_p r_p \rangle \quad (S9)$$

1255 where $\langle \rho_p \rangle$ is the mean particle density of the mass size distribution, $\langle \rho_p r_p \rangle$ is the mean value of (particle density times radius) of the mass size distribution, and r_{eff} is the local effective radius.

S2 Further details on the Self Organizing Maps usage

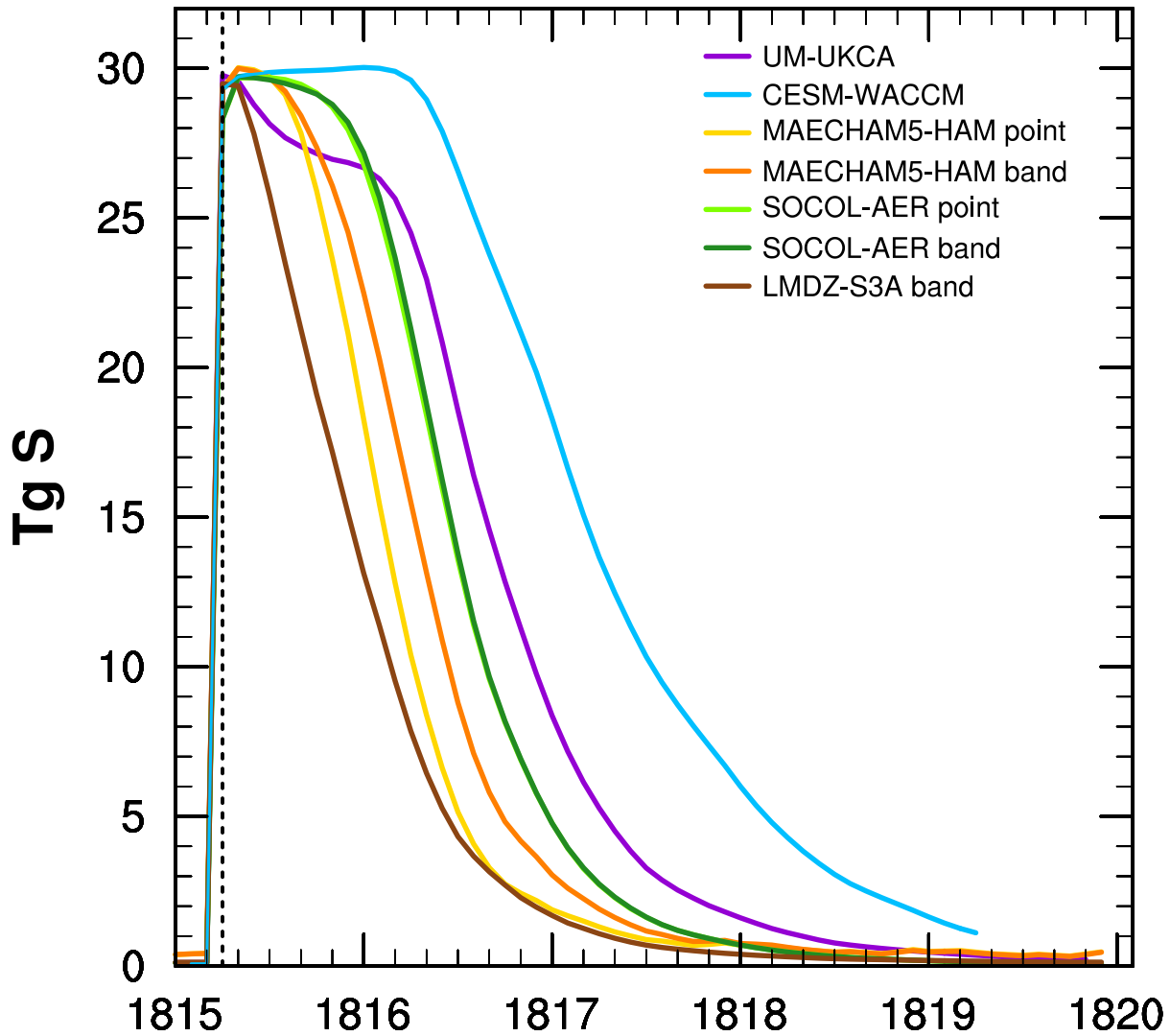
1260 This section of the supplementary info expands on the content in Sect. 4.3.2 of the main text and Appendix D. We wanted to see the similarities and differences in which the models spread the aerosol meridionally in the stratosphere.

For each month, we plotted the meridional (longitudinally averaged) profiles of the stratospheric AOD in each model (Fig. S5). This resulted in 60 plots, with data from 8 models on each plot, giving a total of 480 profiles. Some patterns about how models were circulating the aerosol could be seen by eye, but this was too much data to visualize at once. Next, for each month, each model was normalized by its maximum AOD to better see how the models were circulating the aerosols meridionally (Fig. S6.) 1265 Wanting a better way to visualize how the models were spreading the AOD in terms of latitude and time, we used Self Organizing Maps to reduce the number of squares (months) that were in Fig. S6. The SOM was run over all 60 months for the models, as explained in Appendix D, so the final map was of the most characteristic patterns of normalized AOD versus latitude. The final SOM nodes are plotted as Fig. D1a, and the full results are in Fig. D1. We chose to use the SOM method instead of alternative 1270 machine learning methods because we wanted to see the most characteristic snapshots of the meridional patterns, that still made sense to the eye. Therefore, these patterns did not necessarily have to be orthogonal.

The same process was used on the CESM-WACCM runs for Fig. D2a and Fig. D2b.

1275

Global Stratospheric Sulfur Burden



1280 Figure S1: Global stratospheric burden of sulfur species ($\text{SO}_2 + \text{H}_2\text{SO}_4 + \text{SO}_4$) in TgS vs time for CESM-WACCM (blue), UM-UKCA (purple), SOCOL-AER point (light green), SOCOL-AER band (dark green), MAECHAM5-HAM point (gold) and MAECHAM5-HAM band (orange). Vertical dashed black line indicates month of injection.

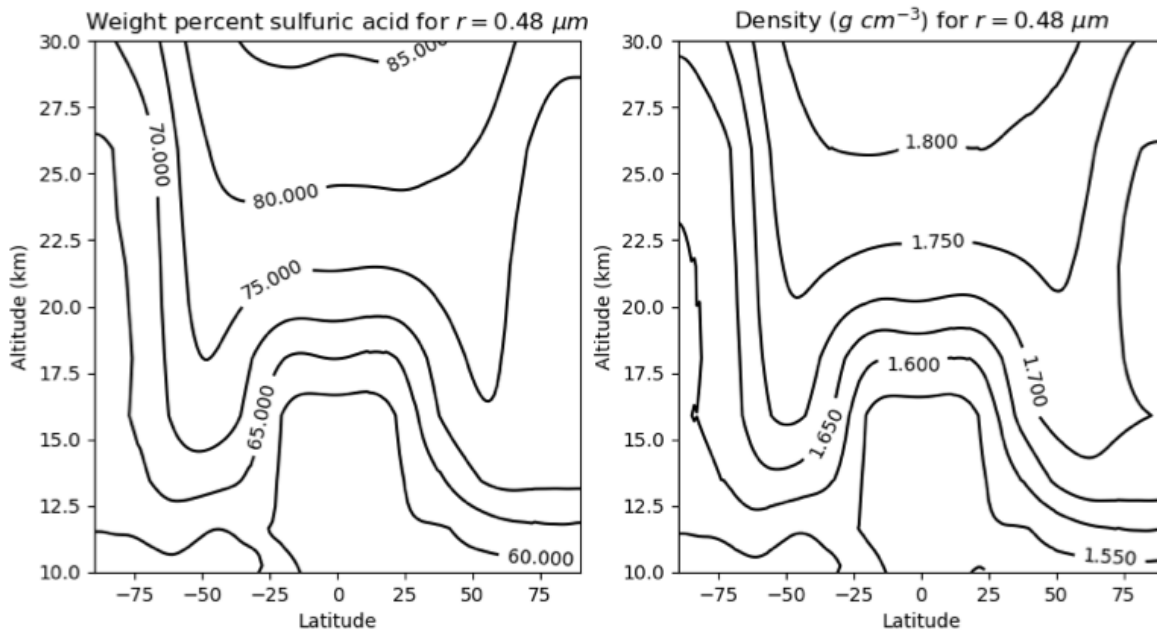


Figure S2: An example of the spatial variation of ω (left) and corresponding ρ (right) from the Community Aerosol and Radiation Model for Atmospheres (CARMA) [Toon et al., 1988]. Figure courtesy of Parker Case.

1285

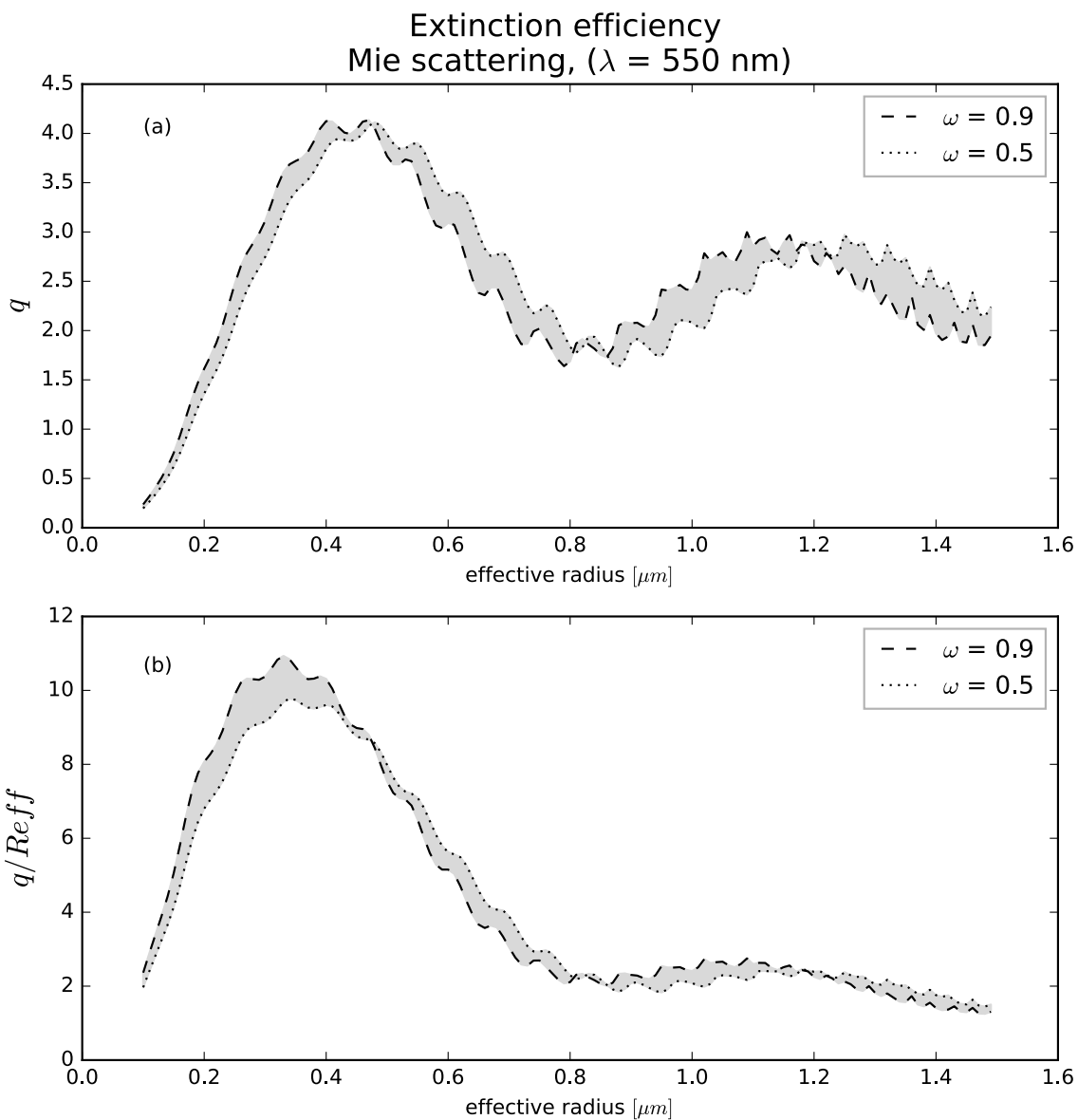
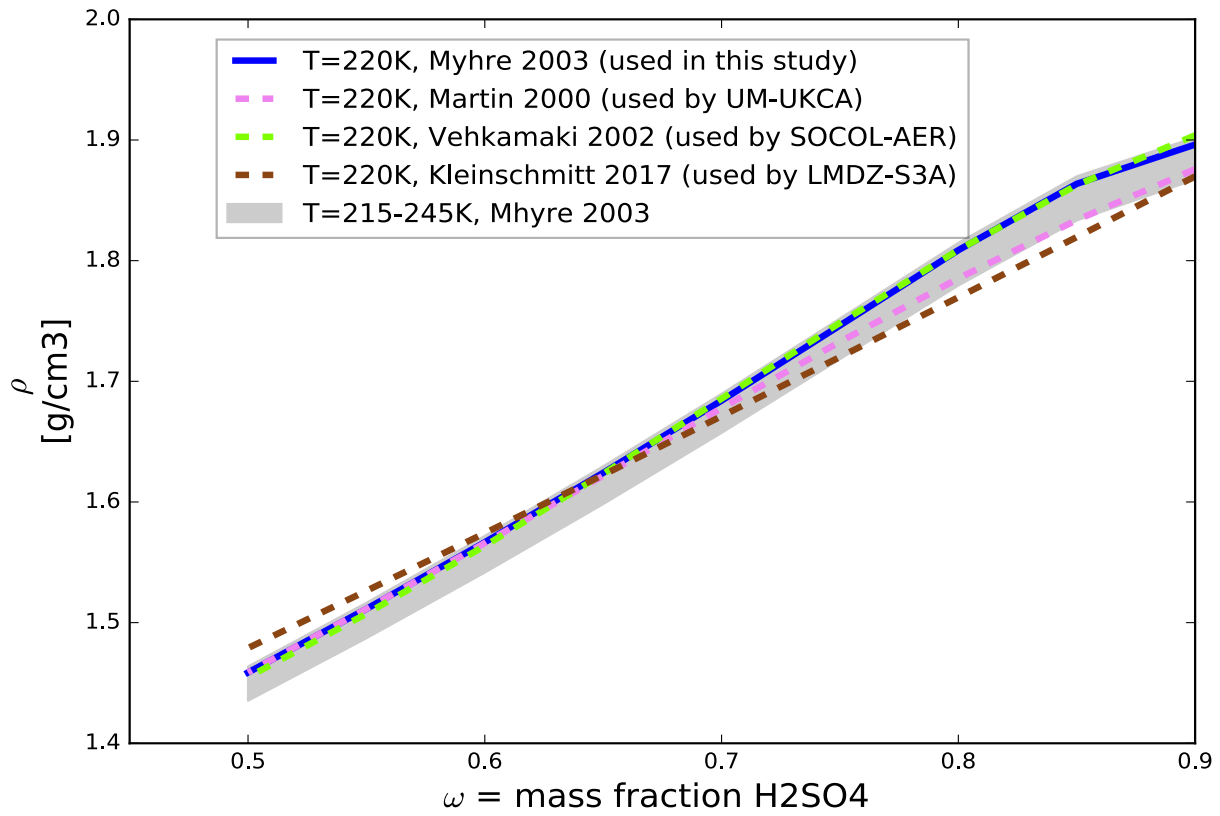


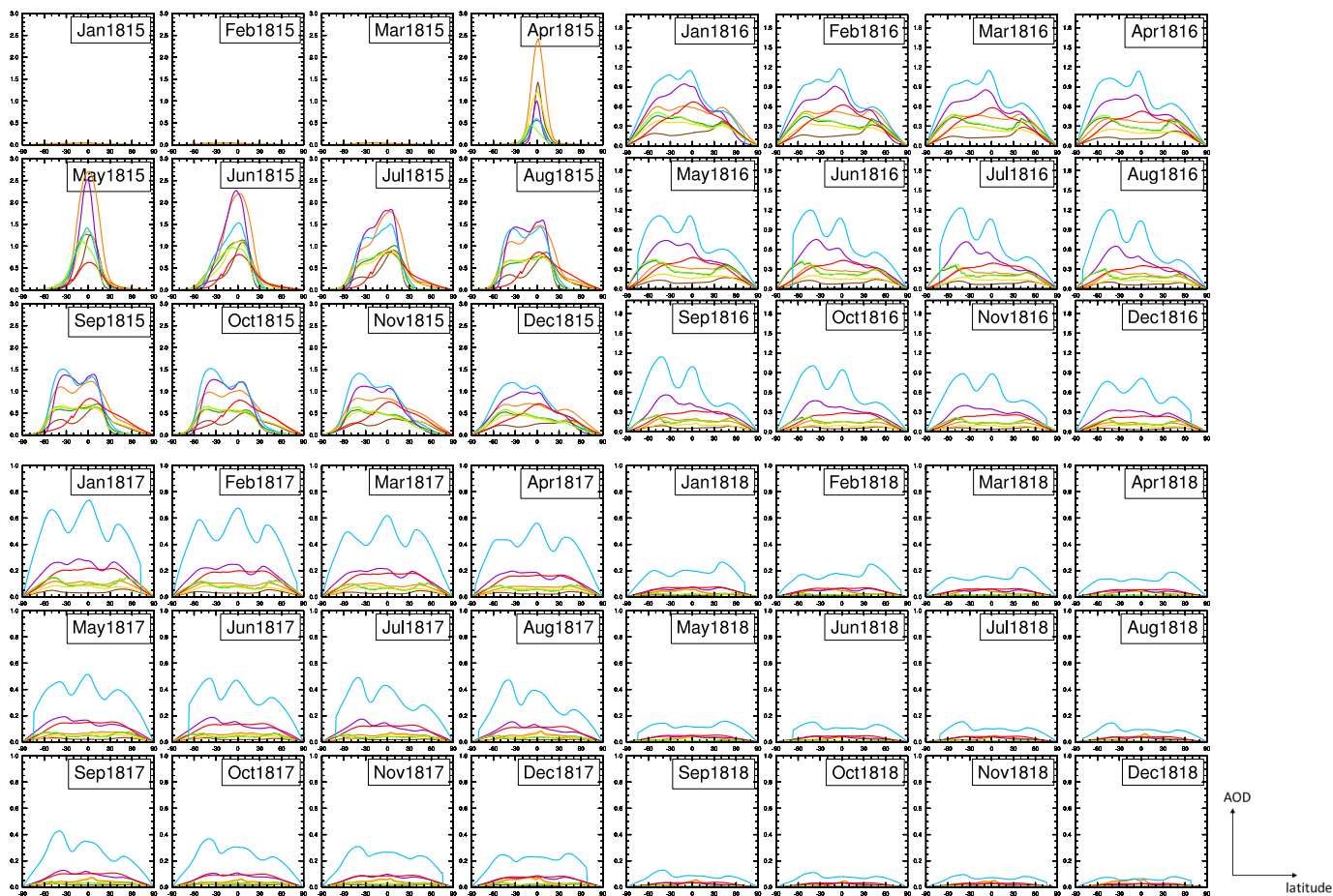
Figure S3: Extinction efficiency (a) and extinction efficiency divided by effective radius (b) from Mie scattering at the visible wavelength of 550nm as a function of effective radius. Values are calculated for q from Mie theory using complex refractive indices corresponding to $\omega = 0.5$ (dotted) through $\omega = 0.9$ (dashed).



1295

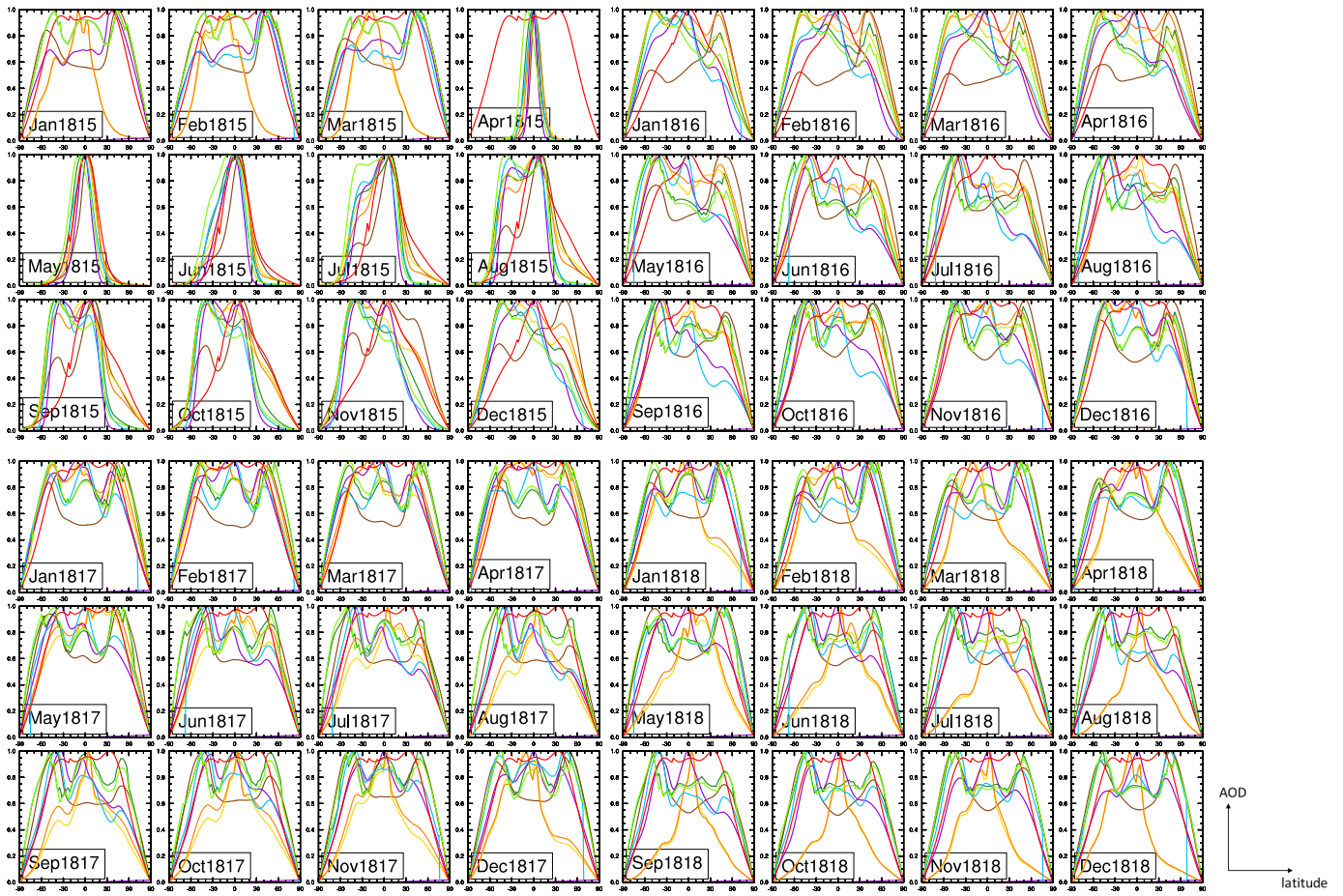
Figure S4: Polynomial functions used by other models to approximate ρ from ω and temperature. Not shown: CESM-WACCM and MAECHAM5-HAM (see Appendix E).

1300



1305

Figure S5: Monthly stratospheric AOD (y-axis) vs Latitude (x-axis with equator at center) for all models. The vertical axis goes from [0, 3.0] for 1815, from [0, 2.0] for 1816, and from [0, 1.0] for 1817 and 1818. The horizontal axis is from [-90, 90]. The eruption occurred in April 1815. Colors correspond to the ensemble mean of the five ensemble runs from CESM-WACCM (blue), UM-UKCA (purple), SOCOL-AER point (lime green), SOCOL-AER band (dark green), MAECHAM5-HAM point (gold), MAECHAM5-HAM band (orange), LMDZ-S3A band (dark brown), and EVA (red).



1310

Figure S6: Normalized monthly stratospheric AOD (y-axis) vs Latitude (x-axis with equator at center) for all models. The vertical axis goes from [0, 1]. The horizontal axis is from [-90, 90]. Colors correspond to the ensemble mean of the five ensemble runs from CESM-WACCM (blue), UM-UKCA (purple), SOCOL-AER point (lime green), SOCOL-AER band (dark green), MAECHAM5-HAM point (gold), MAECHAM5-HAM band (orange), LMDZ-S3A band (dark brown), and EVA (red).

1315